

PET/CT studies of multiple myeloma using ^{18}F -FDG and ^{18}F -NaF: comparison of distribution patterns and tracers' pharmacokinetics

Christos Sachpekidis · Hartmut Goldschmidt · Dirk Hose · Leyun Pan · Caixia Cheng · Klaus Kopka · Uwe Haberkorn · Antonia Dimitrakopoulou-Strauss

Received: 7 December 2013 / Accepted: 29 January 2014 / Published online: 22 February 2014
© Springer-Verlag Berlin Heidelberg 2014

Abstract

Objective The aim of this prospective study is to evaluate the combined use of fluorine-18 fluorodeoxyglucose (^{18}F -FDG) and fluorine-18 sodium fluoride (^{18}F -NaF) PET/CT in the skeletal assessment of patients with multiple myeloma (MM) and to compare the efficacy of these two PET tracers regarding detection of myeloma-indicative osseous lesions.

Patients and methods The study includes 60 patients with multiple myeloma (MM) diagnosed according to standard criteria. All patients underwent dynamic (dPET/CT) scanning of the pelvis as well as whole body PET/CT studies with both

tracers. The interval between the two exams was one day. Sites of focal increased ^{18}F -FDG uptake were considered as highly suspicious of myelomatous involvement. The lesions detected on the ^{18}F -NaF PET/CT scans were then correlated with those detected on ^{18}F -FDG PET/CT, which served as a reference. Moreover, the ^{18}F -FDG PET/CT results were also correlated with the low-dose CT findings. The evaluation of dPET/CT studies was based on qualitative evaluation, SUV calculation, and quantitative analysis based on a 2-tissue compartment model and a non-compartmental approach.

Results Whole body ^{18}F -FDG PET/CT revealed approximately 343 focal lesions while ^{18}F -NaF PET/CT revealed 135 MM-indicative lesions (39 % correlation). CT demonstrated 150 lesions that correlated with those in ^{18}F -FDG PET/CT (44 % correlation). Six patients demonstrated a diffuse pattern of disease with ^{18}F -FDG, while 15 of them had a mixed (diffuse and focal) pattern of skeletal ^{18}F -FDG uptake. A high number of degenerative, traumatic and arthritic disease lesions were detected with ^{18}F -NaF PET/CT. In three patients with multiple focal ^{18}F -FDG-uptake, ^{18}F -NaF PET/CT failed to demonstrate any bone lesion. The dPET/CT scanning of the pelvic area with ^{18}F -FDG and ^{18}F -NaF revealed 77 and 24 MM-indicative lesions, respectively. Kinetic analysis of ^{18}F -FDG revealed the following mean values: $\text{SUV}_{\text{aver}}=5.1$, $k_1=0.37$ (1/min), $k_3=0.10$ (1/min), $V_B=0.06$, $\text{influx}=0.04$ (1/min), $\text{FD}=1.28$; the respective values for ^{18}F -NaF were $\text{SUV}_{\text{average}}=10.7$, $k_1=0.25$ (1/min), $k_3=0.34$ (1/min), $V_B=0.02$, $\text{influx}=0.10$ (1/min), $\text{FD}=1.37$. Apart from the correlation between V_B of ^{18}F -FDG and k_1 of ^{18}F -NaF ($r=0.54$), no other significant correlation was observed between the two tracers' kinetic parameters. We found a significant correlation between FD and $\text{SUV}_{\text{average}}$ ($r=0.93$), FD and SUV_{max} ($r=0.80$), FD and influx ($r=0.85$), as well as between influx and $\text{SUV}_{\text{average}}$ ($r=0.74$) for ^{18}F -FDG. In ^{18}F -NaF we observed the most significant correlations between FD and $\text{SUV}_{\text{average}}$

C. Sachpekidis · L. Pan · C. Cheng · U. Haberkorn · A. Dimitrakopoulou-Strauss
Clinical Cooperation Unit Nuclear Medicine, German Cancer Research Center, Heidelberg, Germany

H. Goldschmidt · D. Hose
Medical Clinic V, University of Heidelberg, Heidelberg, Germany

H. Goldschmidt · D. Hose
National Center for Tumor Diseases Heidelberg, Heidelberg, Germany

K. Kopka
Division of Radiopharmaceutical Chemistry, German Cancer Research Center, Heidelberg, Germany

U. Haberkorn
Division of Nuclear Medicine, University of Heidelberg, Heidelberg, Germany

C. Sachpekidis (✉)
Medical PET Group - Biological Imaging Clinical Cooperation Unit Nuclear Medicine, German Cancer Research Center, Im Neuenheimer Feld 280, 69210 Heidelberg, Germany
e-mail: christos_saxpe@yahoo.gr

C. Sachpekidis
e-mail: c.sachpekidis@dkfz.de

($r=0.97$), FD and SUV_{max} ($r=0.87$), and between influx and k_1 ($r=0.72$).

Conclusion The combined use of ^{18}F -FDG PET/CT and ^{18}F -NaF PET/CT provides different molecular information regarding the biological processes that take place in a MM osseous lesion. ^{18}F -FDG PET/CT proved to be a more specific biomarker than ^{18}F -NaF PET/CT in multiple myeloma skeletal assessment.

Keywords ^{18}F -FDG · ^{18}F -NaF · PET/CT · Multiple myeloma · Compartment analysis

Introduction

Multiple myeloma (MM) is a neoplastic plasma cell disorder, characterized by clonal proliferation of plasma cells in the bone marrow. The diagnosis of MM is based on certain criteria, which comprise the detection of M-protein in the serum and/or urine, bone marrow infiltration by plasma cells and myeloma-related organ or tissue impairment [1]. It is the major plasma cell neoplasm, accounting for approximately 1 % of neoplastic diseases and 13 % of all hematologic malignancies. The skeleton is invaded in almost 80 % of patients resulting in lytic bone lesions [2]. Therefore, imaging assessment of the skeleton is pivotal. The hallmark radiographic lesion of the disease is the focal osteolytic bone lesion [3]. However, an osteolytic lesion occurs after a 30 % involvement of the trabecular bone structure has taken place. Therefore, the application of other imaging modalities that render possible the early detection of tumor burden before irreversible osseous changes take place is needed.

PET and PET/CT technology is becoming more widely available and has nowadays a great impact on tumour diagnostics and management. Although its role is more clarified in solid tumours, PET is gradually becoming more widely acceptable in the evaluation of MM. Dynamic PET (dPET) and PET/CT (dPET/CT) are a modalities that, after application of compartment modelling, enables the acquisition of pharmacokinetic information; this leads to the extraction of values of tracer kinetic parameters, which depict specific molecular processes. Moreover, a non-compartmental model can be applied leading to the estimation of fractal dimension (FD) for the time-activity data, a parameter reflecting heterogeneity. This information is unattainable when the classical whole body PET and PET/CT protocols are performed.

^{18}F -FDG, the workhorse of PET imaging, is a biomarker of intracellular glucose metabolism. The basic concept in its application in MM is that malignant plasma cells, that infiltrate the bone marrow, consume much more glucose than normal cells. ^{18}F -FDG, as a glucose analogue, is taken up by the neoplastic cells, undergoes phosphorylation and then gets trapped intracellularly, since FDG is not a substrate for

further metabolic processing by either phosphohexose isomerase or glucose-6-phosphate dehydrogenase [4]. A number of studies have highlighted the value of ^{18}F -FDG PET in the assessment of MM [5–8]. Moreover, the recently updated Durie/Salmon plus staging system integrates ^{18}F -FDG PET/CT in a MM diagnostic approach [9].

^{18}F -NaF is another PET tracer (positron emitter), early recognized as an excellent radiopharmaceutical for skeletal imaging [10, 11]. However, this agent was replaced during the three previous decades by ^{99m}Tc -MDP bone scintigraphy, performed with the conventional nuclear medicine gamma-cameras. Nevertheless, during recent years the role of ^{18}F -NaF has been revalidated as a highly sensitive and reliable biomarker of bone reconstruction, with potential indications in a wide range of bone diseases [12]. The reason for this re-emergence is the wide availability nowadays of PET and PET/CT scanners and the capability to quantify tracer kinetics. The mechanism of uptake of ^{18}F -NaF is totally different than that of ^{18}F -FDG. The uptake of the tracer in bone occurs by exchange of fluoride with hydroxyl groups in the hydroxyapatite resulting in formation of fluoroapatite [13]. The tracer accumulates in both osteoblastic and osteolytic lesions, reflecting regional blood flow and bone turnover [14]. Little is yet known about the efficiency of ^{18}F -NaF PET/CT in the evaluation of MM. Nishiyama et al., compared the sensitivity of ^{18}F -NaF PET/CT with that of ^{99m}Tc -MDP bone scintigraphy in detecting myeloma lesions in seven MM pts. Their results suggested that the detectability of MM lesions on ^{18}F -NaF PET/CT was promising, but nonspecific [15].

The molecular processes described before, which refer to these two different PET tracers, have been studied and compartmental models have been developed for description of their kinetics. In general, a two-tissue compartmental model can be used for the evaluation of both tracers [14, 16]. These models lead to the extraction of kinetic parameters that describe specific molecular processes, different for each tracer, which will be discussed below. Moreover, a non-compartmental model based on the fractal dimension can be applied for the evaluation of dPET or dPET/CT data, resulting in the extraction of a parameter of heterogeneity (fractal dimension, FD) [17–19].

In the present study, we performed ^{18}F -FDG PET/CT and ^{18}F -NaF PET/CT scanning in patients suffering from MM. The aim of our study was to evaluate the combined use of ^{18}F -FDG PET/CT and ^{18}F -NaF PET/CT in the skeletal assessment of patients with MM and to compare the efficacy of these tracers in detecting MM-indicative lesions. A comparison between the ^{18}F -FDG PET/CT and low-dose CT findings was also performed. Furthermore, we aimed to evaluate, by means of dynamic PET/CT, the pharmacokinetics of these two different PET tracers and detect potential statistically significant correlation between them as well as between parameters of each tracer.

Materials and methods

Patients

The evaluation included 60 patients (37 male, 23 female) confirmed to suffer from MM based on the criteria established by the International Myeloma Working Group [1]. According to the Durie/Salmon staging system, 14 patients were characterized as stage I, five of them as stage II and 41 as stage III of the disease. Their mean age was 59.9 years. The included patients were not diabetic. Forty-six of the patients had primary disease and had never received chemotherapy. Fourteen patients (three in stage II, 11 in stage III) demonstrated recurrent disease; however, none of them had undergone chemotherapy the past six months prior to the dPET/CT studies. Patients gave written informed consent to participate in the study and to have their medical records released. The study was approved by the Ethical Committee of the University of Heidelberg and the Bundesamt für Strahlenschutz.

Data acquisition

The double-tracer study in each patient was completed in two consecutive days. The patients were intravenously administered with a maximum of 250 MBq ^{18}F -FDG on the first day and, respectively, a maximum of 250 MBq ^{18}F -NaF on the second day. Data acquisition consisted of two parts for each tracer: the dynamic part (dPET/CT studies) and the static part (whole body PET/CT). The dPET/CT studies were performed over the pelvic area for 60 minutes using a 28-frame protocol (ten frames of 30 seconds, five frames of 60 seconds, five frames of 120 seconds and eight frames of 300 seconds). The use of lower lumbar spine and pelvic entry for the dynamic series is justified by the fact that this anatomic area is regularly used for diagnostic bone marrow biopsies. Additional whole body static images were acquired in all patients with an image duration of 2 min per bed position for the emission scans. A dedicated PET/CT system (Biograph mCT, 128 S, Siemens Co., Erlangen, Germany) with an axial field of view of 21.6 cm with TruePoint and TrueV, operated in a three-dimensional mode, was used for patient studies. A low-dose attenuation CT (80 kV, 30 mA) was used for the attenuation correction of the dynamic emission PET data and for image fusion. A second low-dose CT (80 kV, 30 mA) was performed after the end of the dynamic series covering the area from the skull to the knees in order to avoid patient movement after the dynamic series. The last images (55–60 minutes post-injection) were used for semi-quantitative analysis. All PET images were attenuation-corrected and an image matrix of 400 x 400 pixels was used for iterative image reconstruction. Iterative images reconstruction was based on the ordered subset expectation maximization algorithm (OSEM) with six iterations and 12 subsets. The reconstructed images were converted to SUV images based on the formula [20]:

$\text{SUV} = \text{tissue concentration (Bq/g)} / (\text{injected dose (Bq)} / \text{body weight (g)})$. The SUVs 55 to 60 minutes postinjection served for the quantification of tracer data.

Data analysis

Data analysis and evaluation was based on: visual analysis of the PET/CT scans, semi-quantitative evaluation based on SUV calculations, and quantitative analysis. Qualitative analysis was based on visual assessment of the PET/CT scans. Two nuclear medicine physicians (CS, ADS) evaluated the hypermetabolic areas on transaxial, coronal, and sagittal images. In particular, skeletal foci presenting with significantly enhanced ^{18}F -FDG uptake, for which another benign aetiology (trauma, inflammation, degenerative changes, arthritic disease, etc.) was excluded, were considered indicative for myeloma. For the minimization of possible false-positive results, the patients' history was studied thoroughly; moreover, the focal ^{18}F -FDG avid lesions were correlated to the fused low-dose CT findings and a comparison between the findings of the two modalities was performed. In particular, we focussed on the evaluation of clearly delineated osteolytic lesions in CT (>8 mm) and compared them with both tracers. Furthermore, patients who demonstrated on maximum intensity projection (MIP) images an intense, homogenous, diffuse increase of bone marrow ^{18}F -FDG uptake were considered as positive for MM involvement (diffuse pattern); the same applied to those patients with a mixed (focal/diffuse) pattern of ^{18}F -FDG uptake. Afterwards, the results of ^{18}F -NaF PET/CT (performed one day later) were correlated to those of ^{18}F -FDG PET/CT, which served as a reference. The basic concept regarding ^{18}F -NaF PET/CT evaluation was that only lesions that correlated with respective lesions on ^{18}F -FDG PET/CT were considered as MM-indicative.

Semi-quantitative evaluation was based on volumes of interest (VOIs), drawn with a 50 % isocontour, placed over foci of increased tracer uptake in the selected area and on subsequent calculation of SUV.

Quantitative evaluation of the dynamic PET/CT data was performed using a dedicated software [21, 22]. Like for SUV calculations, quantitative evaluation was based on irregular VOIs, drawn with a 50 % isocontour, placed over foci of increased radiotracer uptake in the selected osseous area. Time activity curves (TACs) were created using VOIs. It has to be remembered that only lesions located in the anatomic area where dPET/CT was performed (lower lumbar spine and pelvis) were evaluated quantitatively. A detailed quantitative evaluation of tracer kinetics was performed based on a two-tissue compartment model [16, 23, 24]. The input function was retrieved from the image data according to methods already reported in the literature and performed previously by our group [25, 26]. One problem in patients is the accurate measurement of input function. This theoretically requires arterial blood sampling. It has been shown, however, that

input function can be accurately enough retrieved from image data [25]. For the input function, the mean value of the VOI data from a large arterial vessel of the pelvic area (iliac artery) was used. A vessel VOI consisted of at least seven ROIs in sequential PET/CT images. The recovery coefficient was 0.85 for a diameter of 8 mm. Partial volume correction was performed for small vessels (diameter less than 8 mm) based on phantom measurements of the recovery function using dedicated software [21]. The two-tissue compartment model we applied is a modification of the one proposed by Sokoloff et al., which did not take into account the parameters k_4 and V_B [16]. This lack of k_4 and V_B however leads to different values of the parameters k_1 and k_3 , since k_1 is dependent on V_B and k_3 on k_4 . In this study, the constants k_1 to k_4 were calculated taking into account the vascular fraction (V_B) in a VOI as an additional variable. The model parameters were accepted when k_1 - k_4 were less than 1 and V_B exceeded zero. The unit for the rate constants k_1 to k_4 is 1/min, while V_B reflects the fraction of blood within the VOI. Following compartment analysis, we calculated the global influx from the compartment data using the formula: $\text{influx} = (k_1 \times k_3) / (k_2 + k_3)$. In addition to creating VOIs over MM lesions, we also created reference VOIs at the osseous structures of this area (5th lumbar vertebra, os ilium) that didn't demonstrate any focal or intense, diffuse radiotracer accumulation. These areas were considered as negative for myelomatous involvement and served as a reference. The values extracted from these reference areas were then compared to the respective values of MM lesions for potential statistically significant differences.

Besides the compartment analysis, a non-compartment model was used in order to calculate the fractal dimension (FD) for the time-activity data. FD is a parameter of heterogeneity based on the box counting procedure of chaos theory and was calculated for the time activity data in each individual voxel of a VOI. The values of the FD vary from 0 to 2 showing the deterministic or chaotic distribution of the tracer activity. A subdivision of 7 x 7 and a maximal SUV of 20 were applied for the calculation of FD [17].

Data were statistically evaluated using the STATA/SE 12.1 (StataCorp) software on a Intel Core (2.3.06 GHz, 4 GB RAM) running with Mac OS X 10.8.4 (Apple Inc., Cupertino, CA, USA). The statistical evaluation was performed using the descriptive statistics, box plots, Wilcoxon rank-sum test and Spearman's rank correlation analysis. The results were considered significant for p less than 0.05 ($p < 0.05$).

Results

Whole body PET/CT studies

Areas of focal enhanced ^{18}F -FDG uptake were considered to be indicative of myelomatous involvement (MM lesions). As

expected, the number of lesions increased with disease stage. In total, approximately 343 focal ^{18}F -FDG avid skeletal lesions were detected; the 14 stage I pts had six lesions, the five stage II pts had 47 lesions, and the 41 stage III pts demonstrated 290 focal lesions. A correlation between the ^{18}F -FDG and the low-dose CT findings was performed. The comparison revealed 150 circumscribed osteolytic lesions in CT that correlated with the ^{18}F -FDG PET lesions (44 % correlation). In three patients the extent of skeletal disease was very large, rendering the exact calculation of MM lesions practically impossible (innumerable focal lesions). In six patients ($n=4$ stage I, $n=2$ stage III) we observed an intense, diffuse, homogenous increase in ^{18}F -FDG uptake in the bone marrow of the spine, in the os femur, and/or the pelvic bones; 15 patients ($n=1$ stage I, $n=2$ stage II, $n=12$ stage III) demonstrated a mixed (focal/diffuse) pattern of ^{18}F -FDG skeletal uptake. In order to interpret these (diffuse and mixed) patterns of ^{18}F -FDG uptake, we searched the patients' history in order to exclude a reactive phenomenon (e.g., post-chemotherapy reaction); only one patient with diffuse uptake and two with a mixed pattern of ^{18}F -FDG uptake had received chemotherapy in the past. However, none of them had undergone treatment at least six months prior to scanning. Moreover, bone marrow biopsy in patients with diffuse and mixed pattern of ^{18}F -FDG uptake revealed a mean value of 37.8 % and a median value of 43 % regarding plasma cell infiltration rate.

^{18}F -NaF PET/CT demonstrated a generally increased bone uptake. Due to the high sensitivity of the tracer in detecting bone reconstruction, it is difficult to differentiate malignant from benign bone lesions like degenerative, arthritic, traumatic bone disease, etc. Therefore, and as already mentioned, the focal lesions detected on ^{18}F -FDG PET/CT scans were used as reference. Foci of enhanced ^{18}F -NaF uptake were correlated to low-dose CT findings in order to enhance the diagnostic certainty regarding their benign or malignant origin. In general, ^{18}F -NaF PET/CTs demonstrated fewer myeloma-indicative lesions than ^{18}F -FDG PET/CTs. Totally, 135 focal MM lesions were detected with whole body ^{18}F -NaF PET/CT (39 % correlation with ^{18}F -FDG PET/CT). In those MM patients with multiple focal bone lesions in ^{18}F -FDG PET/CT, ^{18}F -NaF PET/CT demonstrated multiple focal lesions in different anatomic areas, not all of which necessarily correlated to ^{18}F -FDG. In three patients with myelomatous skeletal involvement, ^{18}F -NaF PET/CT failed to demonstrate any bone lesion; in 11 of them the number of lesions detected with ^{18}F -NaF was significantly lower than that detected with ^{18}F -FDG.

Interestingly, seven patients with stage III disease didn't demonstrate any focal, diffuse or mixed pattern of increased ^{18}F -FDG uptake. However, CT was also negative for myelomatous lesions in this subgroup. On the other hand, in 15 patients low-dose CT revealed multiple small osteolytic lesions (diffuse involvement) in the axial skeleton mainly,

while PET studies with both tracers were negative; in particular, three patients had multiple small cranial osteolytic lesions, six patients had lesions along the spinal column, four of them in both the skull and the spinal column, one in the humerus, while one in the spine, sternum and pelvis. The results referring to whole body evaluation with both tracers and according to disease stage are presented in Table 1.

Figure 1 demonstrates a characteristic example of a stage III MM patient, who had more skeletal lesions on ¹⁸F-FDG than on ¹⁸F-NaF PET/CT. ¹⁸F-NaF PET/CT detected only three of the multiple osseous MM-indicative lesions that were demonstrated in ¹⁸F-FDG PET/CT.

Figure 2 shows a stage III MM patient, first diagnosed five years ago, who had undergone in the past chemotherapy treatment. The patient had no symptoms at the time of the study. No signs of active myelomatous skeletal involvement are depicted on ¹⁸F-FDG PET/CT. ¹⁸F-NaF PET/CT reveals several positive findings. These represent old fractures, which demonstrate some osteoblastic activity, as well as findings attributed to degenerative and traumatic aetiology. The lesion in the left humerus as well as the lesions in the basis of the skull did not demonstrate any respective correlative findings in the low dose CT.

Figure 3 depicts a stage I MM patient with a diffuse pattern of disease on ¹⁸F-FDG PET/CT. The patient demonstrates a homogenous, diffuse, intense tracer uptake along the spinal column and both femurs.

Dynamic PET/CT studies of the pelvis

In total, 77 MM pelvic lesions were detected with ¹⁸F-FDG dPET/CT and 24 with ¹⁸F-NaF dPET/CT. Table 2 demonstrates the values of the SUVs and kinetic parameters' acquired from the MM lesions with both tracers (mean±SD values). All quantitative data were obtained from VOIs over the focal lesions. The mean values of the MM-lesions' kinetic parameters derived from kinetic analysis, based on ¹⁸F-FDG dPET/CT acquisition, were the following: SUV_{aver}=5.1, SUV_{max}=7.9, k₁=0.37 (1/min), k₃=0.10 (1/min), V_B=0.06, influx=0.04 (1/min), FD=1.28. In comparison, the respective mean values of MM lesions as detected with ¹⁸F-NaF dPET/CT were: SUV_{average}=10.7, SUV_{max}=21.7, k₁=0.25

Table 1 Osseous MM lesions detected with ¹⁸F-FDG and ¹⁸F-NaF according to disease stage

MM stage	No of lesions	
	¹⁸ F-FDG	¹⁸ F-NaF
Stage I (14 pts)	6	3
Stage II (5 pts)	47	9
Stage III (41 pts)	290	123

(1/min), k₃=0.34 (1/min), V_B=0.02, influx=0.10 (1/min), FD=1.37. According to these results, SUVs for ¹⁸F-FDG were significantly lower than for ¹⁸F-NaF. Two-tissue compartment analysis revealed that the parameters k₁ and V_B were significantly lower for ¹⁸F-NaF than for ¹⁸F-FDG; on the contrary, k₃ and influx were significantly higher for ¹⁸F-NaF. The results concerning the between tracers' differences were considered significant for p less than 0.05 (p<0.05). Box plots of k₁, k₃, V_B and influx for both tracers in myelomatous lesions are depicted in Fig. 4. It has to be noted that small MM lesions (8<mm) were not taken into consideration for the dPET/CT evaluations.

Fractal dimension (FD) was applied for further characterization of ¹⁸F-NaF and ¹⁸F-FDG kinetics in MM-indicative foci. The mean FD value was higher for ¹⁸F-NaF, implying a higher degree of heterogeneity of tracer uptake.

We performed a Spearman's rank correlation analysis between ¹⁸F-FDG and ¹⁸F-NaF kinetic parameters: apart from the correlation between V_B of ¹⁸F-FDG and k₁ of ¹⁸F-NaF (r=0.54), no other significant correlation was observed between the two tracers' kinetic parameters. Correlation analysis was also performed between SUVs and kinetic parameters for each tracer separately. In the case of ¹⁸F-FDG, the most significant correlations (p<0.05) were found between FD and SUV_{average} (r=0.93), FD and SUV_{max} (r=0.80), FD and influx (r=0.85), as well as between influx and SUV_{average} (r=0.74) (Table 3). In ¹⁸F-NaF we observed the most significant correlations between FD and SUV_{average} (r=0.97), FD and SUV_{max} (r=0.87), and between influx and k₁ (r=0.72) (Table 4).

We also assessed both tracers' SUVs and kinetic parameters in MM-indicative lesions, in comparison with the respective values of the osseous structures of the pelvis that served as reference. (os ilium, 5th lumbar vertebrae). The comparison was performed after application of the Wilcoxon rank-sum test. This analysis revealed that in the case of ¹⁸F-FDG, all important semi-quantitative and quantitative parameters were significantly higher in MM-lesions than in the reference skeleton (Table 2). On the other hand, in ¹⁸F-NaF, only SUV_{average} and SUV_{max} were significantly higher in myelomatous lesions than in the reference skeleton. All other ¹⁸F-NaF parameters (k₁, k₃, V_B, influx and FD) demonstrated higher mean values in MM lesions than reference areas, but their differences were not statistically significant (p<0.05) (Table 2).

Discussion

Although the routine use of ¹⁸F-FDG PET imaging in MM is still under discussion, it is an undisputable fact that the modality is becoming more widespread and acceptable in diagnostic evaluation and work-up of this malignancy [27]. Moreover, it has been demonstrated that the sensitivity of the

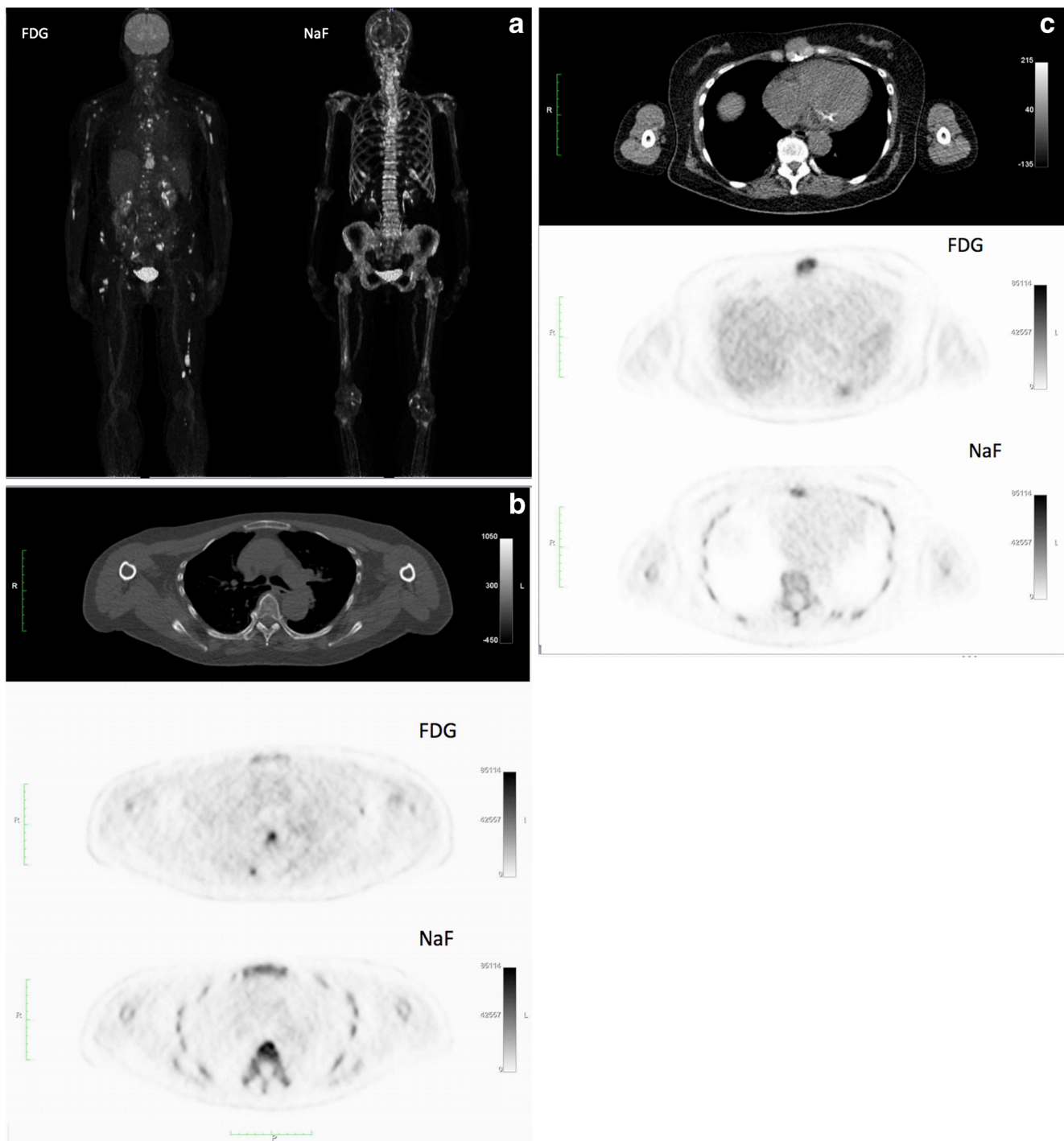


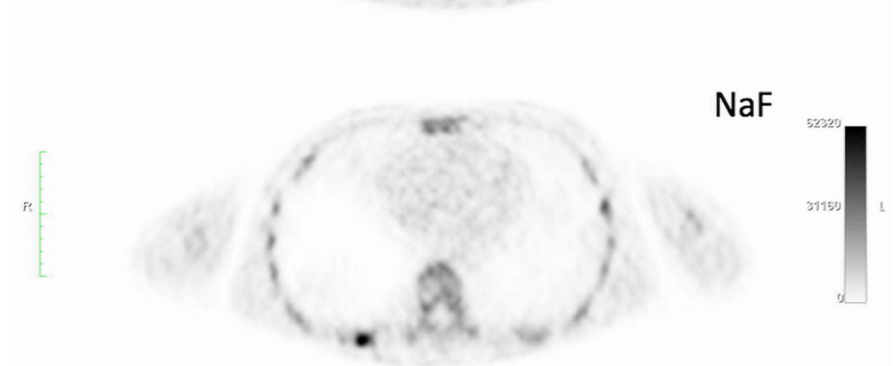
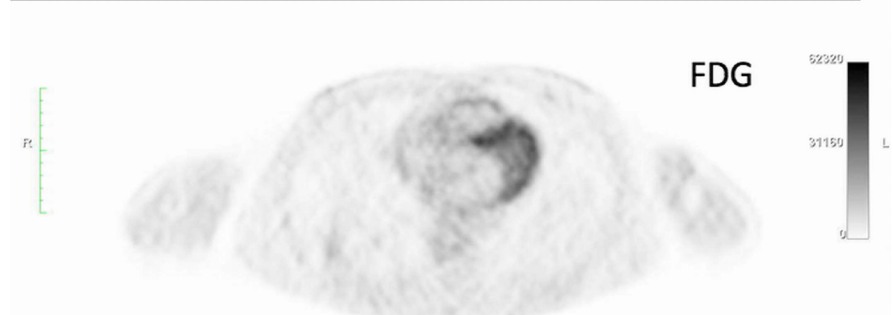
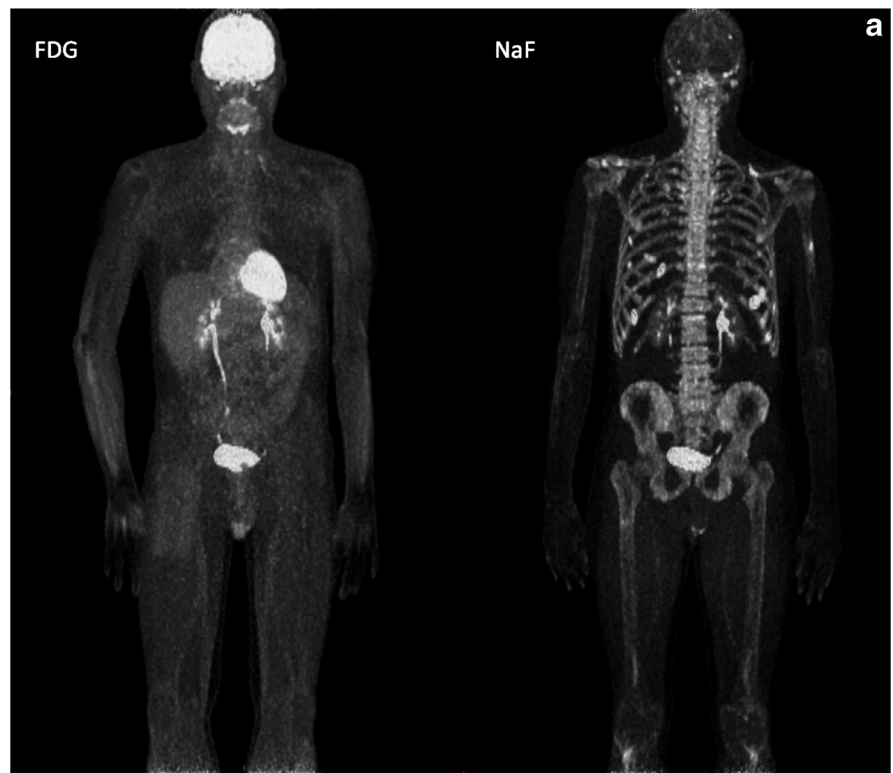
Fig. 1 a: A 69-year-old female stage III MM patient referred to our department for evaluation of extent of skeletal disease with ^{18}F -FDG and ^{18}F -NaF PET/CT. Maximum intensity projection (MIP) revealed multiple hypermetabolic ^{18}F -FDG foci indicative of myelomatous involvement. The respective MIP of ^{18}F -NaF demonstrated much fewer myelomatous indicative lesions. Notice the high number of degenerative lesions depicted on ^{18}F -NaF PET/CT. **b:** CT image of the same patient at the level of the seventh thoracic vertebra, where no osteolysis is depicted

(upper row). Corresponding ^{18}F -FDG PET at the same level, where a site of focal increase tracer uptake is depicted in the seventh thoracic vertebral body (middle row). ^{18}F -NaF PET performed 24 hours later demonstrates no pathological radiotracer accumulation (lower row). Example of ^{18}F -FDG and ^{18}F -NaF “mismatch”. **c:** A sternal lesion of the same patient showing soft tissue infiltration, clearly depicted on CT and ^{18}F -FDG PET, but not demonstrated with ^{18}F -NaF PET (^{18}F -FDG and ^{18}F -NaF “mismatch”)

modality in detecting bone lesions is higher than the standard whole body radiologic skeletal survey [28]. On the other hand,

little is known about the contribution of ^{18}F -NaF PET/CT in the diagnostic approach of the disease. In our study, we tried to

Fig. 2 a: A 48-year-old male stage III MM patient referred to our department for imaging evaluation of the skeleton with ^{18}F -FDG and ^{18}F -NaF PET/CT. The patient was first diagnosed with MM six years ago and had already undergone multiple chemotherapies in the past. At the time of the study he had no signs of active disease, which was consistent with his clinical status. ^{18}F -FDG PET/CT MIP shows no lesions indicative of active myelomatous disease. ^{18}F -NaF PET/CT MIP demonstrates multiple old rib fractures, and other findings due to degenerative changes. **b:** Lesion in the 10th rib due to an old fracture (patient of Fig. 2a). CT shows an osteoblastic lesion due to bone remodelling (upper row). No corresponding radiotracer accumulation depicted on ^{18}F -FDG PET (middle row). ^{18}F -NaF PET demonstrates tracer accumulation indicating the osteoblastic activity (lower row)



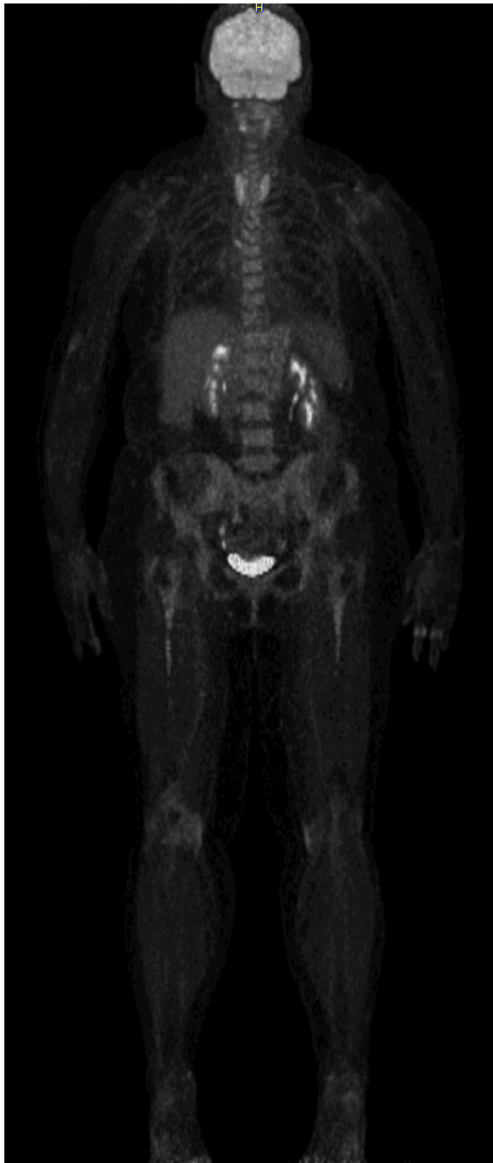


Fig. 3 Diffuse pattern of ^{18}F -FDG bone marrow uptake in a stage I MM patient. The patient demonstrates increased, diffuse uptake along the spinal column and in both femurs. The patient was first diagnosed with MM and had never undergone chemotherapy in the past

evaluate the complementary role of ^{18}F -NaF PET/CT in diagnostic imaging of MM patients. The study was comprised of two parts: the whole body PET/CT evaluation with the use of the two different PET tracers ^{18}F -FDG and ^{18}F -NaF, and the dPET/CT part in which we compared the kinetics of ^{18}F -FDG with the kinetics of ^{18}F -NaF. As already mentioned, the MM-indicative lesions detected on ^{18}F -FDG PET/CT were the reference on which the lesions detected with ^{18}F -NaF were correlated and compared. However, all lesions detected on ^{18}F -NaF PET/CT were studied thoroughly. A comparison between the ^{18}F -FDG PET and low-dose CT findings was also performed.

Table 2 Descriptive statistics of SUVs and kinetic parameters for ^{18}F -FDG and ^{18}F -NaF in MM bone lesions and reference bone tissue. The values refer to mean \pm SD. k_1 , k_3 and influx expressed in (1/min)

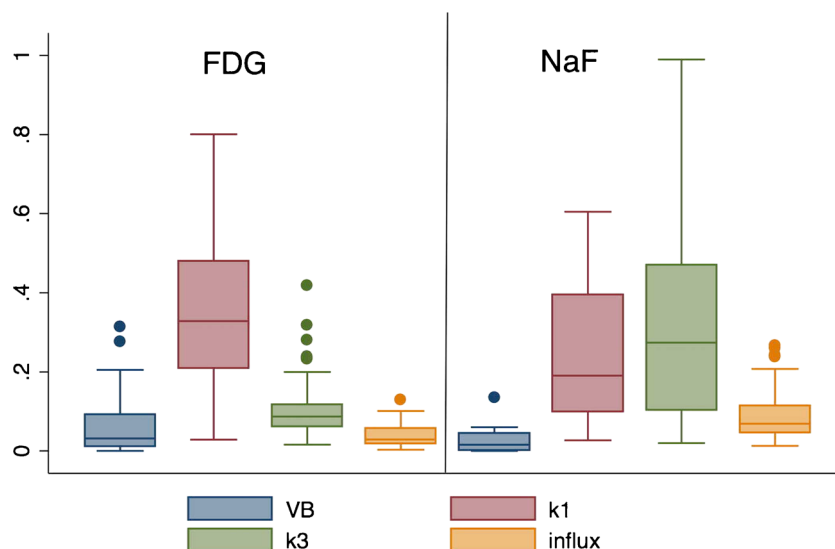
Radiopharmaceutical	Parameters	MM lesions	reference tissue
^{18}F -FDG	SUV _{aver} *	5.1 \pm 2.2	1.8 \pm 0.8
	SUV _{max} *	7.9 \pm 3.8	3.2 \pm 1.6
	k_1 *	0.37 \pm 0.20	0.22 \pm 0.10
	k_3 *	0.10 \pm 0.07	0.05 \pm 0.04
	V_B *	0.06 \pm 0.06	0.02 \pm 0.03
	influx*	0.04 \pm 0.03	0.01 \pm 0.01
	FD*	1.28 \pm 0.08	1.10 \pm 0.10
^{18}F -NaF	SUV _{aver} *	10.7 \pm 5.9	7.9 \pm 2.5
	SUV _{max} *	21.7 \pm 20.6	13.3 \pm 5.1
	k_1	0.25 \pm 0.19	0.21 \pm 0.11
	k_3	0.34 \pm 0.29	0.28 \pm 0.19
	V_B	0.02 \pm 0.03	0.02 \pm 0.03
	influx	0.10 \pm 0.08	0.08 \pm 0.03
	FD	1.37 \pm 0.08	1.36 \pm 0.06

* significant probabilities ($p < 0.05$)

M-W test Mann-Whitney test for the probability of differences between the two groups “MM lesions” and “reference tissue”

Whole body PET/CT imaging with these two PET tracers leads us to the conclusion that in general terms ^{18}F -FDG is a more reliable biomarker than ^{18}F -NaF in the evaluation of MM: The number of MM lesions detected with ^{18}F -FDG was significantly higher than that detected with ^{18}F -NaF. In addition, although ^{18}F -FDG is a non-specific tracer, its number of false-positive findings (based on low dose CT and patients’ history) was much smaller than the false-positive findings detected with ^{18}F -NaF. The reason for this, is the accumulation of ^{18}F -NaF in every site of newly mineralizing bone, irrelevant of its aetiology; this means that any cause of bone reconstruction (e.g., traumatic, degenerative bone lesions) will lead to ^{18}F -NaF accumulation. It is actually impossible to differentiate a malignant from a benign bone lesion with ^{18}F -NaF PET alone. The correlation with other imaging modalities like CT or MRI, as well as a detailed patient’s history are required, as realized in our study. In particular, most positive rib findings in ^{18}F -NaF, which did not have any ^{18}F -FDG correlation were attributed – after correlation with CT - to traumatic aetiology (old fractures) or may represent old myelomatous lesions that still accumulated ^{18}F -NaF due to persistent increased osteoblastic activity; furthermore, degenerative changes like osteophytes in the spinal column or arthritis (primarily in the joints of the knees and hips) could be easily interpreted as “non-myelomatous lesions”. Our results demonstrated that ^{18}F -NaF PET/CT didn’t actually aid in MM diagnostic evaluation. Its main contribution was that it gave a general view of the bone remodelling of the whole skeleton. As already mentioned, ^{18}F -FDG PET/CT did not demonstrate

Fig. 4 Box plots of ¹⁸F-FDG and ¹⁸F-NaF kinetic parameters k_1 , k_3 , V_B and influx in MM lesions. The data demonstrate that k_3 and influx of ¹⁸F-NaF are significantly higher than in ¹⁸F-FDG, while V_B and k_1 are higher for ¹⁸F-FDG than for ¹⁸F-NaF ($p < 0.05$)



any enhanced accumulation (focal, diffuse or mixed) in seven patients suffering from stage III MM. However, this shouldn't be considered as a limitation of the modality in detecting MM skeletal lesions, since other myeloma-related organ or tissue impairment (such as renal insufficiency, anaemia, hypercalcaemia, etc.) could lead to patient classification in a high disease stage. This is also supported by the fact that these patients also didn't demonstrate any osteolytic lesions in the low-dose CT.

The second part of our study investigated the kinetics of ¹⁸F-FDG in MM osseous lesions and compared them with the kinetics of ¹⁸F-NaF in respective lesions, as these were derived from dPET/CT studies of the pelvic skeleton.

A two-tissue compartment model was used for the evaluation of dPET/CT studies with both tracers. The use of the two-tissue compartment model is a generally accepted approach for the assessment of ¹⁸F-FDG kinetics; the application of this model leads to the extraction of the kinetic parameters $k_1 - k_4$, influx (K_i) and fractional blood volume (V_B), also called vessel density, which correlates to blood volume in the VOI. Briefly, in the case of ¹⁸F-FDG k_1 reflects the influx while k_2 reflects the efflux of the radiopharmaceutical, and k_3 represents the phosphorylation rate while k_4 the

dephosphorylation rate of the glucose analogue. Influx (K_i) is derived from the equation $= (k_1 \times k_3) / (k_2 + k_3)$. The application of the two-tissue compartment model in ¹⁸F-NaF leads also to the extraction of kinetic parameters [14]. However, these parameters reflect different molecular mechanisms than ¹⁸F-FDG. In the case of ¹⁸F-NaF, rate constants k_1 and k_2 describe the fluoride ions exchange with hydroxyl groups of hydroxyapatite crystal of the bone and the reverse, while k_3 and k_4 represent the formation of fluoroapatite and the opposite [24]. Influx K_i is related to Ca^{2+} influx and bone apposition rate and, presumably, represents bone remodelling rate [29]. We compared the kinetic parameters ($k_1 - k_4$, V_B , influx) and SUVs for ¹⁸F-FDG and ¹⁸F-NaF using multivariate analysis; with the exception of the correlation between V_B of ¹⁸F-FDG and k_1 of ¹⁸F-NaF ($r=0.54$), no other significant correlation was found for $k_1 - k_4$ and SUVs between the two tracers. The data indicate that the rate constants $k_1 - k_4$ are tracer specific and provide different molecular information. Correlation analysis performed for each tracer separately demonstrated the very high correlation between FD and $SUV_{average}$ and SUV_{max} in both tracers. Furthermore, we found a highly significant correlation ($r=0.74$) between the influx and

Table 3 Results of the Spearman's rank correlation analysis between MM lesions' quantitative and semi-quantitative (SUVs) parameters of ¹⁸F-FDG. Values were considered significant for $p < 0.05$

	SUV _{average}	SUV _{maximum}	k_1	k_3	V_B	influx	FD
SUV _{average}							
SUV _{maximum}	0.8500*						
k_1	0.3694	0.1290					
k_3	0.4999*	0.5181*	-0.3214*				
V_B	0.3690*	0.2523	0.4254*	0.2020			
influx	0.7357*	0.5605*	0.5812*	0.4394*	0.4947*		
FD	0.9283*	0.7954*	0.5651*	0.3937*	0.4590*	0.8523*	

*significant correlation ($p < 0.05$)

Table 4 Results of the correlation analysis between MM lesions' quantitative and semi-quantitative (SUVs) parameters of ^{18}F -NaF. Values were considered significant for $p < 0.05$

	SUV _{average}	SUV _{maximum}	k_1	k_3	V_B	influx	FD
SUV _{average}							
SUV _{maximum}	0.8878*						
k_1	0.3183	0.3522					
k_3	0.6252*	0.4026	0.1991				
V_B	-0.2235	-0.1661	0.0000	-0.4087*			
influx	0.6513*	0.5417*	0.7217*	0.5070*	-0.0835		
FD	0.9687*	0.8661*	0.3304	0.5548*	-0.1826	0.6217*	

*Significant correlation ($p < 0.05$)

SUV_{aver} in ^{18}F -FDG. This finding is in accordance with respective results derived from kinetic ^{18}F -FDG PET studies in other tumors. Strauss et al., reported a correlation of 0.76 ($p < 0.01$) between SUV_{aver} and the influx in primary colorectal cancers [26]. We also noted a significant but lower correlation ($r = 0.65$) between SUV_{average} and the nflux in ^{18}F -NaF.

Our group has previously shown that the application of dynamic quantitative ^{18}F -FDG PET has a high accuracy in differentiation of malignant and benign bone lesions. In particular, that study showed that all kinetic parameters (with the exception of k_2 and k_4) and SUVs were higher in malignant bone tumors than in benign ones. Moreover the t test revealed significantly higher mean values of SUV, V_B , influx and FD in malignant than benign tumors ($p < 0.05$) [30]. In the present study, we compared the SUVs and kinetic parameters of both ^{18}F -FDG and ^{18}F -NaF in multiple myeloma lesions with the respective parameters of reference osseous tissue. The results of our study showed that in the case of ^{18}F -FDG, the MM-indicative bone lesions demonstrated SUVs and kinetic parameters' values that ranged in significantly higher levels than the reference skeleton. In contradiction to the results of ^{18}F -FDG kinetic analysis, in the case of ^{18}F -NaF only SUV_{average} and SUV_{max} were statistically significantly higher in MM-indicative lesions than the reference skeleton; all other parameters (k_1 , k_3 , V_B , influx and FD) didn't reveal significant differences between lesions and reference tissue. These data support our basic conclusion that ^{18}F -NaF is not a specific tracer for malignancy detection in MM patients. Due to its very high sensitivity for bone reconstruction detection, it is difficult to differentiate between malignant and benign lesions only based on the ^{18}F -NaF PET results, even after the application of quantitative analysis. Moreover, it is possible for an initially positive lesion in both tracers to become ^{18}F -FDG negative following chemotherapy, but to demonstrate a prolonged ^{18}F -NaF uptake, due to persistent surrounding osteoblastic activity.

In addition to applying a two-tissue compartment model for evaluation of tracers' kinetics, a non-compartmental approach was also performed leading to the extraction of another index that is representative of tissue heterogeneity, FD. This parameter is based on the box counting procedure of the chaos theory for the analysis of dPET data [17]. The basic concept

is that an increased FD is indicative of a more chaotic tracer distribution, correlating to a higher tissue heterogeneity. In the present study, the FD values in MM-lesions were comparable with a median of 1.28 for ^{18}F -FDG and 1.37 for ^{18}F -NaF. Furthermore, as already mentioned, FD demonstrated a highly significant correlation with SUV_{average} both in ^{18}F -FDG ($r = 0.93$) as well as in ^{18}F -NaF studies ($r = 0.97$). This is in accordance with previous studies showing that both FD for the time-activity data and SUV's are enhanced in malignancies [17]. It is our belief that the application of this non-compartment derived parameter can be useful in evaluation of complicated oncological differential diagnosis issues.

A limitation of this study is the lack of histological confirmation for myelomatous osseous lesions. In clinical practice, however, it is not possible to confirm by histology every MM-indicative lesion. In fact, only the correlation to other imaging modalities, like CT and MRI, and the patient's clinical outcome serve as a reference. Another limitation is the use of low dose CT, which was performed for the anatomical assignment of the lesions and for attenuation correction.

Conclusion

In recent years, the role of PET/CT with ^{18}F -FDG in diagnostic evaluation of MM has been upgraded. ^{18}F -NaF is another PET tracer, which serves as a highly sensitive and reliable biomarker of bone reconstruction and with potential indications in a wide range of bone diseases. We aimed to study the combined use of these two PET tracers in the diagnostic work-up of patients with MM. The results of our study imply that the additional PET/CT scanning with ^{18}F -NaF doesn't add significant information to the diagnostic approach of MM patients, who have already gone through ^{18}F -FDG PET/CT. However, ^{18}F -NaF provides general information regarding bone remodelling and the patient's skeletal history.

Acknowledgements This study is part of the Sonderforschungsbereich-Transregio 79 (SFB-TRR 79) and was financially supported by the Deutsche Forschungsgemeinschaft (German Research Foundation, DFG).

Conflict of interest The authors declare that they have no conflict of interest.

References

- International Myeloma Working Group. Criteria for the classification of monoclonal gammopathies, multiple myeloma and related disorders: a report of the International Myeloma Working Group. *Br J Haematol.* 2003;121:749–57.
- Palumbo A, Anderson K. Multiple myeloma. *N Engl J Med.* 2011;364:1046–60.
- Walker RC, Brown TL, Jones-Jackson LB, De Blanche L, Bartel T. Imaging of multiple myeloma and related plasma cell dyscrasias. *J Nucl Med.* 2012;53:1091–101.
- Mason NS, Lin EC. Basics of fluorodeoxyglucose radiochemistry and biology. In: Lin EC, Alavi A (eds). *PET and PET/CT: a clinical guide.* Thieme medical publisher, Inc 2005; p.15-20.
- Durie BG, Waxman AD, D'Agnolo A, Williams CM. Whole-body (18)F-FDG PET identifies high-risk myeloma. *J Nucl Med.* 2002;43:1457–63.
- Schirmeister H, Bommer M, Buck AK, Müller S, Messer P, Bunjes D, et al. Initial results in the assessment of multiple myeloma using 18 F-FDG PET. *Eur J Nucl Med Mol Imaging.* 2002;29:361–6.
- Bredella MA, Steinbach L, Caputo G, Segall G, Hawkins R. Value of FDG PET in the assessment of patients with multiple myeloma. *AJR Am J Roentgenol.* 2005;184:1199–204.
- Fonti R, Larobina M, Del Vecchio S, De Luca S, Fabbriolini R, Catalano L, et al. Metabolic tumor volume assessed by 18 F-FDG PET/CT for the prediction of outcome in patients with multiple myeloma. *J Nucl Med.* 2012;53:1829–35.
- Durie BG. The role of anatomic and functional staging in myeloma: description of Durie/Salmon plus staging system. *Eur J Cancer.* 2006;42:1539–43.
- Blau M, Ganatra R, Bender MA. 18 F-Fluoride for bone imaging. *Semin Nucl Med.* 1972;2:31–7.
- Grant FD, Fahey FH, Packard AB, Davis RT, Alavi A, Treves ST. Skeletal PET with 18 F-fluoride: applying new technology to an old tracer. *J Nucl Med.* 2008;49:68–78.
- Segall G, Delbeke D, Stabin MG, Even-Sapir E, Fair J, Sajdak R, et al. SNM. SNM practice guideline for sodium 18 F-fluoride PET/CT bone scans 1.0. *J Nucl Med.* 2010;51:1813–20.
- Schiepers C, Nuyts J, Bormans G, Dequeker J, Bouillon R, Mortelmans L, et al. Fluoride kinetics of the axial skeleton measured in vivo with fluorine-18-fluoride PET. *J Nucl Med.* 1997;38:1970–6.
- Hawkins RA, Choi Y, Huang SC, Hoh CK, Dahlbom M, Schiepers C, et al. Evaluation of the skeletal kinetics of fluorine-18-fluoride ion with PET. *J Nucl Med.* 1992;33:633–42.
- Nishiyama Y, Tateishi U, Shizukuishi K, Shishikura A, Yamazaki E, Shibata H, et al. Role of 18 F-fluoride PET/CT in the assessment of multiple myeloma: initial experience. *Ann Nucl Med.* 2013;27:78–83.
- Sokoloff L, Smith CB. Basic principles underlying radioisotopic methods for assay of biochemical processes in vivo. In: Greitz T, Ingvar DH, Widén L, editors. *The metabolism of the human brain studied with positron emission tomography.* New York: Raven Press; 1983. p. 123–48.
- Dimitrakopoulou-Strauss A, Strauss LG, Burger C, Mikolajczyk K, Lehnert T, Bernd L, et al. On the fractal nature of positron emission tomography (PET) studies. *World J Nucl Med.* 2003;4:306–13.
- Dimitrakopoulou-Strauss A, Pan L, Strauss LG. Quantitative approaches of dynamic FDG-PET and PET/CT studies (dPET/CT) for the evaluation of oncological patients. *Cancer Imaging.* 2012;12:283–9.
- Pan L, Mikolajczyk K, Strauss L, Haberkorn U, Dimitrakopoulou-Strauss A. Machine learning based parameter imaging and kinetic modeling of PET data. *J Nucl Med.* 2007;48:158p.
- Strauss LG, Conti PS. The applications of PET in clinical oncology. *J Nucl Med.* 1991;32:623–48.
- Burger C, Buck A. Requirements and implementations of a flexible kinetic modeling tool. *J Nucl Med.* 1997;38:1818–23.
- Mikolajczyk K, Szabatin M, Rudnicki P, Grodzki M, Burger C. A Java environment for medical image data analysis: initial application for brain PET quantitation. *Med Inform.* 1998;23:207–14.
- Miyazawa H, Osmont A, Petit-Taboué MC, Tillet I, Travère JM, Young AR, et al. Determination of 18 F-fluoro-2-deoxy-D-glucose rate constants in the anesthetized baboon brain with dynamic positron tomography. *J Neurosci Methods.* 1993;50:263–72.
- Cheng C, Alt V, Dimitrakopoulou-Strauss A, Pan L, Thormann U, Schettler R, et al. Evaluation of new bone formation in normal and osteoporotic rats with a 3-mm femur defect: functional assessment with dynamic PET-CT (dPET-CT) using a 2-deoxy-2 [(18)F] fluorodeoxyglucose (18 F-FDG) and 18 F-fluoride. *Mol Imaging Biol.* 2013;15:336–44.
- Ohtake T, Kosaka N, Watanabe T, Yokoyama I, Moritan T, Masuo M, et al. Noninvasive method to obtain input function for measuring tissue glucose utilization of thoracic and abdominal organs. *J Nucl Med.* 1991;32:1432–8.
- Strauss LG, Klippel S, Pan L, Schönleben K, Haberkorn U, Dimitrakopoulou-Strauss A. Assessment of quantitative FDG PET data in primary colorectal tumours: which parameters are important with respect to tumour detection? *Eur J Nucl Med Mol Imaging.* 2007;34:868–77.
- Bird JM, Owen RG, D'Sa S, Snowden JA, Pratt G, Ashcroft J, et al. Guidelines for the diagnosis and management of multiple myeloma 2011. *Br J Haematol.* 2011;154:32–75.
- van Lammeren-Venema D, Regelink JC, Riphagen II, Zweegman S, Hoekstra OS, Zijlstra JM. 18 F-fluoro-deoxyglucose positron emission tomography in assessment of myeloma-related bone disease: a systematic review. *Cancer.* 2012;15(118):1971–81.
- Czernin J, Satyamurthy N, Schiepers C. Molecular mechanisms of bone 18 F-NaF deposition. *J Nucl Med.* 2010;51:1826–9.
- Dimitrakopoulou-Strauss A, Strauss LG, Heichel T, Wu H, Burger et al. The role of quantitative (18)F-FDG PET studies for the differentiation of malignant and benign bone lesions. *J Nucl Med.* 2002;43:510–8.